

# Nonequilibrium Ionization States of Gamma-Ray Burst Environments

|       |   |
|-------|---|
| メタデータ | 言語: eng<br>出版者:<br>公開日: 2017-10-03<br>キーワード (Ja):<br>キーワード (En):<br>作成者:<br>メールアドレス:<br>所属: |
| URL   | <a href="https://doi.org/10.24517/00010304">https://doi.org/10.24517/00010304</a>           |

This work is licensed under a Creative Commons Attribution-NonCommercial-ShareAlike 3.0 International License.



## NONEQUILIBRIUM IONIZATION STATES OF GAMMA-RAY BURST ENVIRONMENTS

DAISUKE YONETOKU,<sup>1,2</sup> TOSHIO MURAKAMI,<sup>1,2</sup> KUNIAKI MASAI,<sup>3</sup> ATSUMASA YOSHIDA,<sup>4</sup>  
NOBUYUKI KAWAI,<sup>2</sup> AND MASAAKI NAMIKI<sup>5</sup>

Received 2001 May 9; accepted 2001 July 9; published 2001 July 26

### ABSTRACT

Iron spectral features are thought to be the best tracers of progenitors of gamma-ray bursts (GRBs). The detections of spectral features such as an iron line and/or the radiative recombination edge and continuum (RRC) were reported in four X-ray afterglows of GRBs. However, burst for burst, their properties were different from each other. For example, the *Chandra* observation of GRB 991216 detected a strong H-like iron line together with the RRC. With *ASCA*, on the other hand, Yoshida and coworkers detected only the strong RRC in GRB 970828. Since it is difficult to produce the strong RRC, we have to consider a special condition for the line- and/or RRC-forming regions. In this Letter, we point out the possibility of a “nonequilibrium ionization state” for the line- and RRC-forming regions.

*Subject headings:* gamma rays: bursts — line: formation — X-rays: general

### 1. INTRODUCTION

Gamma-ray bursts (GRBs) are remote at cosmological distances, and thus their released energies in gamma-ray photons are almost  $\sim 10^{52}$  ergs (Kulkarni et al. 1999). Although fireball models (Rees & Mészáros 1992; Piran 1999) or a cannonball model (Dar & De Rújula 2000) can explain many observational properties of GRBs, a progenitor of a GRB is yet to be solved. An important key to probing a progenitor of a GRB is the detection of iron spectral features in X-ray afterglows. Iron is the most abundant heavy element and falls in the middle of the observed energy range of X-ray satellites. Strong iron features can be produced in a dense gas environment. Therefore, the detection is the best evidence of a collapsing model of a massive star such as a hypernova/collapsar or a supranova (Paczynski 1998; Woosley 1993; Vietri & Stella 1998).

The iron features were already reported in four X-ray afterglows. The redshifted iron emission line was discovered in the X-ray afterglow of GRB 970508 by Piro et al. (1999) using *BeppoSAX*, and the redshift was consistent with the distance of a host galaxy. An independent discovery of a redshifted iron emission line was reported for GRB 970828 by Yoshida et al. (1999) using *ASCA*. Assuming an He-like  $K\alpha$  line, the spectral feature was once interpreted as an emission line with a redshift of  $z = 0.33$ . However, the Keck observation of the host galaxy, which was discovered later in 1998, revealed a redshift of  $z = 0.9578$  (Djorgovski et al. 2001). The discrepancy in distance with *ASCA* and, moreover, the temporal detections of both caused us to doubt the reality of the existence of the iron features before the confirmation by the *Chandra* detection.

In 1999, with the ACIS-S/HETG instruments, *Chandra* detected GRB 991216, 37 hr after the GRB, and Piro et al. (2000) reported the detection of both the iron emission line and the

radiative recombination edge and continuum (RRC) from fully ionized iron with a high statistical significance of  $4.7 \sigma$  and  $3.0 \sigma$ , respectively. The redshift of the line and the RRC were consistent with the host galaxy, and the line was broadened to  $\sigma_{\text{line}} = 0.23 \pm 0.07$  keV, suggesting a moving ejecta. Soon after the *Chandra* detection, Antonelli et al. (2000) also reported the probable iron emission line in the spectrum of GRB 000214 with an  $\sim 3.2 \sigma$  confidence level. This was the second detection of the iron using *BeppoSAX*. However, the redshift of the host galaxy of GRB 000214 is unknown. Therefore, it remains a question whether the observed feature is the iron emission line or the RRC.

Motivated by the RRC detection with *Chandra*, Yoshida et al. (2001, hereafter Paper I) apply the RRC to the *ASCA* data of GRB 970828 using a redshift of  $z = 0.9578$  and obtain the edge energy, which is consistent with 9.28 keV. This possibility was earlier suggested in the paper by Djorgovski et al. (2001). However, there was no iron  $K\alpha$  line detected at the expected energy from GRB 970828. The upper limit of the line flux is less than  $1.5 \times 10^{-6}$  photons  $\text{cm}^{-2} \text{s}^{-1}$  or 120 eV in equivalent width (EW). We must explain the nondetection of the  $K\alpha$  line.

Related to the iron features, we should note that the iron features were only found in a small fraction ( $<10\%$ ) of X-ray afterglows, and sometimes the features were observed only during a certain interval. With *BeppoSAX*, we have tried to search lines in 11 X-ray afterglow spectra, but only one from GRB 970508 was found at the end of 1999 (L. Piro 1999, private communication). Most X-ray afterglows showed only upper limits. In particular, with *ASCA* Yonetoku et al. (2000) set an extremely low upper limit of almost 100 eV in EW for the bright GRB 990123. The published intensities of the observed iron  $K\alpha$  line and the RRC are summarized in Table 1. There is a wide variety in the iron emission and the RRC intensity. In this Letter, we try to explain these varieties of the iron features with the assumption that the line-emitting plasma state is in a “nonequilibrium ionization (NEI) state” that has a low electron temperature as compared with the ionization degree.

### 2. SPECTRAL SIMULATION FOR NONEQUILIBRIUM PLASMA

In Paper I, the observed flux of the RRC and the upper limit for the iron  $K\alpha$  line are given for GRB 970828 with 90% confidence errors. Therefore, we focus on the ratio of the in-

<sup>1</sup> Institute of Space and Astronautical Science, 3-1-1, Yoshinodai, Sagami-hara, Kanagawa 229-8510, Japan; yonetoku@astro.isas.ac.jp, murakami@astro.isas.ac.jp.

<sup>2</sup> Department of Physics, Tokyo Institute of Technology, 2-12-1, Ookayama, Meguro, Tokyo 152-0033, Japan.

<sup>3</sup> Department of Physics, Tokyo Metropolitan University, 1-1, Minamiosawa, Hachioji, Tokyo 192-0397, Japan.

<sup>4</sup> Department of Physics, Aoyama Gakuin University, 6-16-1, Chitosedai, Setagaya, Tokyo 157-8572, Japan.

<sup>5</sup> Institute of Physical and Chemical Research, 2-1, Hirosawa, Wako, Saitama 351-0198, Japan.

TABLE 1  
INTENSITY OF IRON LINE AND RRC

| GRB                       | $z$   | $F_{\text{line}}$<br>(photons $\text{cm}^{-2} \text{s}^{-1}$ ) | $\sigma$<br>(keV) | $F_{\text{RRC}}$<br>(photons $\text{cm}^{-2} \text{s}^{-1}$ ) | $kT$<br>(keV)       |
|---------------------------|-------|--|-------------------|---|---------------------|
| 970508 <sup>a</sup> ..... | 0.835 | $(3.0 \pm 2.0) \times 10^{-5}$                                 | ...               | ...   | ...                 |
| 970828 <sup>b</sup> ..... | 0.958 | $<1.5 \times 10^{-6}$  | ...               | $1.7_{-1.2}^{+6.4} \times 10^{-5}$                            | $0.8_{-0.2}^{+1.0}$ |
| 991216 <sup>c</sup> ..... | 1.020 | $(3.2 \pm 0.8) \times 10^{-5}$                                 | $0.23 \pm 0.07$   | $3.8 \pm 2.0$   | $>1.0$              |
| 000214 <sup>d</sup> ..... | ...   | $(9 \pm 3) \times 10^{-6}$                                     | ...               | ...   | ...                 |
| 990123 <sup>e</sup> ..... | 1.600 | $<3.3 \times 10^{-6}$  | ...               | ...   | ...                 |
| 990704 <sup>e</sup> ..... | ...   | $<4.7 \times 10^{-6}$  | ...               | ...   | ...                 |

<sup>a</sup> The line intensity was variable (Piro et al. 1999).

<sup>b</sup> The RRC was temporal (Paper I).

<sup>c</sup> Piro et al. 2000.

<sup>d</sup> Antonelli et al. 2000.

<sup>e</sup> Yonetoku et al. 2000.

tegrated RRC flux to the iron intensity  $F_{\text{RRC}}/F_{\text{line}}$ , which is free from the continuum. The observed ratio of  $F_{\text{RRC}}/F_{\text{line}} > 3.3$  in a 90% statistical lower limit is very hard to reproduce. The case of a strong RRC without a  $K\alpha$  line looks abnormal. In fact, *BeppoSAX* detected the strong  $K\alpha$  line, and the *Chandra* observation showed both features of the H-like iron with the flux ratio  $F_{\text{RRC}}/F_{\text{line}} \sim 1$ . Therefore, we are forced to consider a different condition between *ASCA* and other results containing the strong  $K\alpha$  line.

The nondetection of the  $K\alpha$  line of highly ionized iron accompanied by the recombination edge gives us a constraint on the possible emission mechanisms. If the line were produced because of the excitation by an electron impact, the RRC would be hidden by a much more intense thermal bremsstrahlung. Also, the synchrotron emission, which is thought to dominate the afterglow, would be significantly overlaid by the thermal bremsstrahlung. Therefore, we need a condition in which the iron is highly ionized but in which the involved electron energy is low. This would be a radiative recombination in the NEI ( $T_e < T_z$ ) state; otherwise, the charge exchange would be responsible for the iron emission.

In this section, we show spectra using numerical calculations in the NEI plasma state and not depending on the specific model. To explain the observed strong RRC without the  $K\alpha$  line of iron, we calculate the emissivity using the NEI plasma radiation code (Masai 1994). The code employs three mechanisms for the continuum: free-free emission, 2 photon decay, and radiative recombination. For line emissions as well as for excitation by electron impact, fluorescent lines due to ionization and cascade lines due to recombination are taken into account. The radiation properties of a plasma were described by two parameters of the electron temperature ( $T_e$ ) and the ionization degree represented in units of temperature ( $T_z$ ), assuming a cosmical abundance. We study the emissivities in the range of  $0.1 \text{ keV} < kT_e < 10 \text{ keV}$  and  $0.1 \text{ keV} < kT_z < 100 \text{ keV}$  in every  $0.1 \text{ keV}$  step. We show representative spectra in Figure 1.

The strong RRC compared with the  $K\alpha$  line can be formed only in the regime of  $T_e < T_z$ , recombining the plasma condition. This condition, however, is attained by several situations that will be discussed later. We intend to find the condition of the plasma in order to account for the observed flux ratio ( $F_{\text{RRC}}/F_{\text{line}}$ ), which is free from specific modeling with iron abundance, the emission measure, the geometry, and so forth if the line and RRC are emitted from the same site. Thus, for a given  $T_e$  and  $T_z$  a priori, we carried out calculations of the emissivity ratio in the above wide range of  $T_e$ - $T_z$  space.

Figures 1c and 1d are the simulated plasma emissivities with a cosmical abundance explaining the ratio  $F_{\text{RRC}}/F_{\text{line}}$  of GRB

991216 and GRB 970828, respectively. The ratios of an integrated RRC flux to  $K\alpha$  lines of the simulated ionization state are  $F_{\text{RRC}}/F_{\text{line}} \sim 1$  and  $\sim 4$  for Figures 1c and 1d, respectively, and the ratios are within the observational values in a 90% statistical error. In the calculation of the ratios, the line components (mostly a blend of Fe and Ni) very close to the edge of the RRC are included in the RRC component because of the limited energy-resolving power of the Solid-State Imaging Spectrometer (SIS) on board *ASCA*.

### 3. THE REASON FOR STRONG RRC AND WEAK $K\alpha$ LINE

To produce the strong RRC in quantum number  $n = 1$ , the iron must be almost fully ionized. The H-like  $K\alpha$  line, which was observed with *Chandra*, dominates other ionization states at a temperature of  $kT_z > 20 \text{ keV}$ . Above this temperature, Fe xxvii consists of more than 70% iron; thus, we assume that  $kT_z > 20 \text{ keV}$  in the following discussion. In a condition with a high electron temperature of  $kT_e \sim kT_z > 20 \text{ keV}$ , i.e., equilibrium ionization, the capture rate of free electrons is small, and the emissivity of the line and the RRC also becomes small. Moreover, the free-free emission from high- $T_e$  electrons dominates at the hard X-ray band. Therefore, the RRC may not be observed because it can be obscured by the free-free component.

The cross section of the electron capture into the  $n$ th quantum state can be expressed as

$$\sigma_n \propto \frac{1}{n^3} \left( \frac{3kT_e}{2\epsilon} + \frac{1}{n^2} \right)^{-1}, \quad (1)$$

where  $\epsilon$  is an ionization energy of 9.28 keV for H-like iron (e.g., Nakayama & Masai 2001). Thus, the best condition to form the strong RRC would be the case of  $kT_e \sim \epsilon (\ll kT_z)$ . In such a plasma state,  $\sigma_n \propto n^{-3}$ , and then most of the free electrons recombine directly into the ground state ( $n = 1$ ), compared with the  $n \geq 2$  levels. However, free-free emission dominates the continuum.

With decreasing  $kT_e$ , the recombination rate increases, while free-free emission becomes suppressed. Recombination into  $n \geq 2$  increases relatively and produces line emission. Thus, the  $K\alpha$  line can be enhanced by cascades from  $n \geq 3$  excited levels. This is the case for He-like  $K\alpha$ , but H-like  $K\alpha$  ( $\text{Ly}\alpha$ ) is little affected; a considerable fraction comes to direct transition to the ground state.

We summarize the above discussions in view of the intensity of the RRC and  $K\alpha$  line. The plasma state with the strong RRC but a weak  $K\alpha$  line, which was observed with *ASCA*, is realized

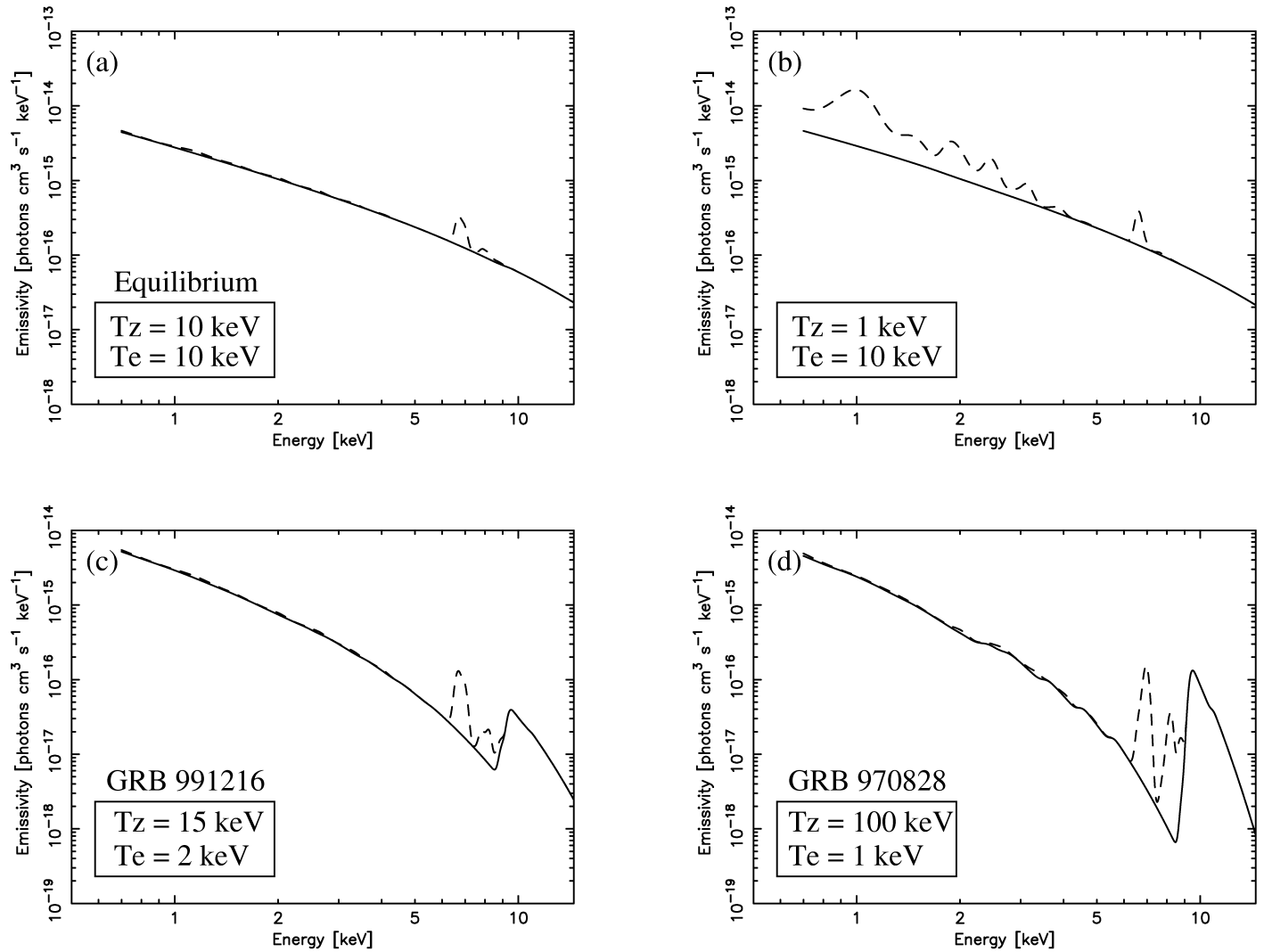


FIG. 1.—Simulated emissivities convolved with the energy resolution of the ASCA SIS for the following cases: (a)  $T_z = 10$  keV,  $T_e = 10$  keV (equilibrium); (b)  $T_z = 1$  keV,  $T_e = 10$  keV; (c)  $T_z = 15$  keV,  $T_e = 2$  keV; and (d)  $T_z = 100$  keV,  $T_e = 1$  keV. The solid lines represent the emissivity of the continuum, and the dashed lines represent the emission lines. Panels c and d are simulated to represent the cases of GRB 991216 and GRB 970828, respectively, but only in view of the observed ratios of  $F_{\text{RRC}}/F_{\text{line}}$ . We do not intend to reproduce the spectral shapes, which mostly consist of a nonthermal component.

when  $kT_e$  is slightly less than  $\epsilon$  but in high  $kT_z$ . The ratio of the RRC to  $K\alpha$  lines ( $F_{\text{RRC}}/F_{\text{line}}$ ) from the numerical calculations is shown in Figure 2 as a function of  $T_e$  and  $T_z$ . The peak of the ratio appears at around  $kT_e = 4$  keV and  $kT_z = 100$  keV in the calculated range. The condition of  $F_{\text{RRC}}/F_{\text{line}} > 3.3$  of GRB 970828 can be explained by this result.

#### 4. DISCUSSION

A high-ionization degree of  $kT_z \sim 100$  keV and a low electron temperature of  $kT_e \sim 1$  keV are required when we reproduce the high ratio of the RRC to the iron line of more than 3.3. This condition may be attained in (1) the photoionizations by X-rays or (2) the rapid cooling due to rarefaction.

Case 1 is also likely accompanied by a fluorescent  $K\alpha$  line with 6.4–6.5 keV energies of partially ionized iron. In particular, for the photoionizations of a neutral circumstellar gas by the initial bright flash of a GRB, iron lines in the low-ionization states are expected but not observed. The line observed using *Chandra* was purely H-like (Piro et al. 2000). Therefore, the iron atoms should be fully ionized by the time of the observed iron emission. However, if the line- and RRC-emitting regions

are illuminated continuously by a hidden intense beam, discussed by Rees & Mészáros (2000), they can achieve the NEI ( $T_e < T_z$ ) state by the photoionization process. Even if this process is realized, the mean energy of the hidden-beam photons that illuminate the line-emitting region should not be significantly greater than the edge energy of 9.28 keV since the observed values of  $T_e$  were low;  $kT_e = 0.8_{-0.2}^{+1.0}$  keV at the rest frame for ASCA and  $kT_e \gtrsim 1$  keV for *Chandra*.

In case 2, we pay attention to the rapid adiabatic expansion of a highly ionized hot plasma. This sort of mechanism has already been investigated by Itoh & Masai (1989) for a supernova exploded in the circumstellar matter that was ejected during its progenitor's supergiant phase. They show that when the blast shock breaks out of the dense circumstellar matter into a low-density interstellar medium, a rarefaction wave propagates inward into the shocked hot plasma. Then the hot plasma expands adiabatically and loses its internal energy quickly. The electron temperature  $T_e$  decreases, but the ionization degree  $T_z$  temporally remains high, because the recombination timescale becomes much longer as a result of the low density. The mean temperature of the shocked matter,  $kT \sim 100(v_s/10^9 \text{ cm s}^{-1})^2$  keV, where  $v_s$

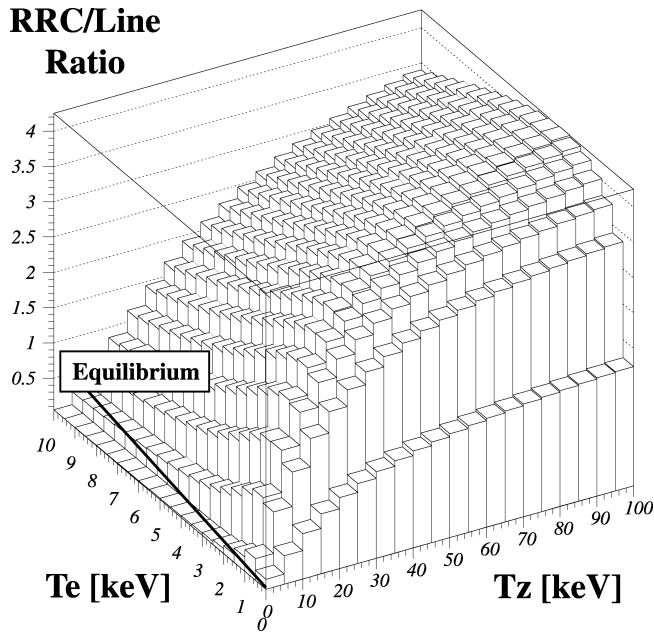


FIG. 2.—Ratios of the integrated emissivity of the RRC structure to the  $K\alpha$  lines ( $F_{\text{RRC}}/F_{\text{line}}$ ) for several ionization states in a three-dimensional axis. We calculate the ratio of the emissivity for each  $T_z = 5$  keV and  $T_e = 0.5$  keV step. The thick solid line labeled “equilibrium” indicates the condition of  $T_e = T_z$ . The recombination process is only enhanced in the  $T_e < T_z$  region. Within our calculated range, the observed ratio of  $F_{\text{RRC}}/F_{\text{line}} > 3.3$  for GRB 970828 can be attained in the range of more than  $T_z = 80$  keV, limiting the  $T_e = 1$  keV, which is observed in the RRC structure.

is the shock velocity, drops by about 2 orders of magnitude for the density contrast (ratio) of the dense matter to the ambient medium of  $\sim 10^3$  in their hydrodynamic calculations. Therefore, the plasma can achieve the NEI ( $T_e \sim 1$  keV,  $T_z \sim 100$  keV) state naturally and can emit the strong RRC with a weak  $K\alpha$  line of  $F_{\text{RRC}}/F_{\text{line}} \sim 4$ .

If these mechanisms work, we can estimate an emission measure for GRB 970828 using the observed photon flux of the RRC ( $F_{\text{RRC}}$ ), the distance ( $D$ ) and the integrated emissivity ( $\epsilon_{\text{RRC}}$ ), shown in Figure 2, with the cosmical abundance,

$$n^2 V \sim 10^{68} \left( \frac{D}{3 \text{ Gpc}} \right)^2 \left( \frac{F_{\text{RRC}}}{1.7 \times 10^{-5}} \right) \left( \frac{\epsilon_{\text{RRC}}}{2 \times 10^{-16}} \right)^{-1}. \quad (2)$$

Although these  $n$  and  $V$  are coupled with each other and depend highly on the specific model, we may conclude that the density of line-emitting region is considerably high.

The RRC and/or the line of a large EW suggest a recombined ( $T_e < T_z$ ) condition, which can be realized by photoionization or rarefaction. It should be noted that most of the X-ray afterglow did not show both emission features; the NEI state is not always the case.

We would like to thank Shri Kulkarni and George Djorgovski for their comments and suggestions about the distance to the host galaxy before publication. This work was done under the support of a Grant-in-Aid for Scientific Research (12640302) by the Ministry of Education, Culture, Sports, Science, and Technology.

#### REFERENCES

- Antonelli, L. A., et al. 2000, *ApJ*, 545, L39  
 Dar, A., & De Rújula, A. 2000, *A&A*, submitted (astro-ph/0008474)  
 Djorgovski, S. G., et al. 2001, *ApJ*, submitted  
 Itoh, H., & Masai, K. 1989, *MNRAS*, 236, 885  
 Kulkarni, S., et al. 1999, *Nature*, 398, 389  
 Masai, K. 1994, *ApJ*, 437, 770  
 Nakayama, M., & Masai, K. 2001, *A&A*, in press  
 Paczyński, B. 1998, *ApJ*, 494, L45  
 Piran, T. 1999, *Phys. Rep.*, 314, 575  
 Piro, L., et al. 1999, *ApJ*, 514, L73  
 Piro, L., et al. 2000, *Science*, 290, 955  
 Rees, M. J., & Mészáros, P. 1992, *MNRAS*, 258, 41P  
 ———. 2000, *ApJ*, 545, L73  
 Vietri, M., & Stella, L. 1998, *ApJ*, 507, L45  
 Woosley, S. E. 1993, *ApJ*, 405, 273  
 Yonetoku, D., et al. 2000, *PASJ*, 52, 509  
 Yoshida, A., Namiki, M., Otani, C., Kawai, N., Murakami, T., Ueda, Y., Shibata, R., & Uno, S. 1999, *A&AS*, 138, 433  
 Yoshida, A., et al. 2001, *ApJ*, 557, L000 (Paper I)